Passive Thermal Management of a Lithium-Ion Battery Using Carbon Fiber Loaded Phase Change Material: Comparison and Optimization

Ahmadi Mezjani, Mehdi; Karimi, Gholam Reza
Department of Chemical Engineering, Shiraz University, Shiraz, I.R. IRAN

Medi, Bijan
Department of Chemical Engineering, Hamedan University of Technology, Hamedan, I.R. IRAN

Babapoor, Aziz*+; Paar, Meysam
Department of Chemical Engineering, University of Mohaghegh Ardabili, Ardabil, I.R. IRAN

ABSTRACT: *Phase Change Materials (PCMs) are currently used for many heat management applications. However, the heat transfer performance of PCMs is limited by their low thermal diffusivities. This is a critical issue for high heat flux applications, such as in the thermal management of lithium-ion (Li-ion) batteries. The present work aims the study heat transfer enhancement in a cylindrical Li-ion battery thermal management system consisting of a PCM (paraffin) loaded with randomly distributed and radially oriented carbon fibers. The system was simulated numerically under various cooling conditions, including naturally convecting air, in the presence of pure paraffin, and the presence of carbon fiber-loaded paraffin. The results for orderly arranged carbon fibers were compared with those of random distribution. Numerical results indicated that better battery thermal management can be achieved for the radially distributed carbon fiber arrangement in the PCM. The advantage of radial over random distributions can be due to the constant, uniform, and non-agglomerating distribution of carbon fibers under which thermo-physical properties of carbon fibers are better realized in the composite medium. The presence of carbon fibers with thermal conductivity of k=50W/m K in the PCM has caused more uniform temperature profiles in the radial direction because of the improved thermal conductivities. The results of this research can be used as a guideline for designing a battery thermal management system.*

KEYWORDS: *Li-ion battery; Phase Change Material (PCM); Carbon fiber; Composite; Radial arrangement.*

INTRODUCTION

Lithium-ion (Li-ion) batteries are an inseparable part of modern life. Numerous electrical appliances ranging from simple toys to high-tech satellites are powered by Li-ion batteries. The discharging as well as charging of

***** *To whom correspondence should be addressed.*
+ *E-mail*: *babapoor@uma.ac.ir & babapoor2006@yahoo.com*
1021-9986/2022/1/310-327 18/$/6.08

Li-ion batteries are typically associated with heat effects [1]. The generated heat during a battery discharge (or charge) must be adequately dissipated to the surroundings to avoid damage or even the occurrence of dangerous runaway reactions within the battery chemical matrix [1]. For sensitive and advanced applications such as electric vehicle systems, the generated heat is typically removed by a thermal management system [2, 3]. An excellent thermal management system must maintain the battery in a predefined temperature range**.**

In recent years, Phase Change Materials (PCMs) have been used as one of the promising cooling media for thermal management of Li-ion batteries [4]. Phase change materials can absorb or release a large quantity of latent heat during a phase change (from solid to liquid or vice versa). Among various PCMs commonly used in thermal energy storage systems, paraffin waxes are more favorable due to their availability, chemical stability, durability to cycling, and reasonable cost. Paraffin also has a range of melting points suitable for the thermal control of batteries and portable electronics. However, one of the main paraffin's drawbacks is its low thermal conductivity/diffusivity, which slows down its capability for heat transfer. To alleviate this issue, materials with higher thermal conductivities such as metal nanoparticles, metal matrices, graphite, and carbon fibers are typically added to PCM at various compositions [5-17]. Among recently developed materials, PCM composites have offered lots of advantages because of their combination of thermophysical and mechanical characteristics, including high thermal conductivity, stable form, and resistance to oxidation [18-25].

Applications of PCMs in the thermal management of Li-ion batteries have been studied by many researchers in the past few years. *Al-Hallaj et al.* [26] proposed different kinds of PCMs for thermal management of Li-ion batteries employed in plug-in hybrid vehicles. *Khateeb et al.* [27] used PCM composites containing aluminum foam for thermal management of a Li-ion battery. They reported more uniform temperature distribution within the battery and a 50% drop in the maximum battery temperature. Carbon fibers have also been added to PCMs to promote heat transfer. *Fukai et al.* [28] used random and brush types of carbon fibers to enhance the thermal conductivity of energy storage media. It was shown that the brush-type fibers could increase the effective thermal conductivities to the maximum values predicted theoretically.

Haghighi et al. [29] investigated the effect of adding different weight percentages of various nanoparticles, such as CuO, TiO_2, Al_2O_3, and graphene to paraffin for the improvement of the thermal properties of PCM. The results showed that the nanocomposites containing 2 wt.% and 1 wt.% graphene nanocomposite had the highest and lowest energy storage capacity compared to paraffin, respectively. The results indicated that Nano-Enhanced Phase Change Materials (NEPCMs) could be particularly useful in applications in which temperature control is crucial. *Cao et al.* [30] used composites, including Paraffin Wax (PW), Expanded Graphite (EG), High-Density PolyEhylene (HDPE), Carbon Fiber (CF), and a 3D printed aluminum honeycomb with a prickly structure (3D Al-Hc). The Composite PCM (CPCM) was applied to a battery cooling module to determine the temperature response of a battery. The results showed that when the CF mass fraction was 4.5 wt.%, the degree of supercooling in the PW/EG/CF/HDPE composite was reduced by 51.5% and 43.3% compared to PW/PCM and PW/EG CPCM, respectively.

Frusteri et al. [31] evaluated the effect of carbon fibers loading on the thermal conductivity enhancement of an inorganic PCM (eutectic mixture of $Mg(NO_3)_2.6H_2O$–$MgCl_2.6H_2O$–NH_4NO_3 as a PCM). Recently, *Samimi et al.* [32] have shown that the presence of carbon fibers in the paraffin mixture can significantly improve the effective thermal conductivity of a cooling medium used for a Li-ion battery. Various carbon fiber length and weight fractions have been used in the study, and considerable thermal conductivity enhancements have been reported.

Karimi and *Li* [33] and *Karimi* and *Dehghan* [34, 35] used fundamental heat transfer principles and performance characteristics of commercial Li-ion batteries to predict temperature distributions in a typical battery pack filled with PCM under a wide range of discharge and flow configuration conditions. They showed that PCM could potentially control the cell-to-cell temperature distribution within the desired range.

In one review by *Al-Hallaj et al.* [36], it was shown that the technology base for PCM-integrated in the battery module is available in a relatively simple design, and thereby provides appreciable cost reduction compared to active cooling systems. *Javani et al.* [37] have applied a finite volume-based numerical model to investigate the thermal management of an electric vehicle battery pack using PCM. The effect of different operating conditions

on the thermal performance of the sub-module was examined with and without the presence of the PCM. A more uniform temperature distribution was observed when PCM was employed.

Despite a large number of investigations conducted for thermal management of Li-ion batteries, there are still many unanswered questions related to the effective use of heat transfer promoters with the PCMs, especially those which involve carbon fibers. In the present study, the thermal performance of a cylindrical Li-ion battery cell is simulated using Computational Fluid Dynamics (CFD) under various cooling medium conditions, which are naturally convecting air, the presence of pure paraffin, and the presence of carbon fiber loaded paraffin wax. The effect of carbon fiber mass fraction, as well as the distribution patterns on the temperature profiles, was investigated. In practice, the random dispersion of carbon fibers in the PCM can be associated with an agglomeration of carbon fibers and hence inefficient temperature dispersion within the composite as pointed out in [32]. However, the radial distribution of highly conductive materials such as carbon fiber improves heat transfer in the r-direction. This is a very important feature that synergistically enhances the heat transfer from the battery to the surrounding environment. Overall, this condition improves heat transfer in the composite phase change material. It must be emphasized that the radial placement of carbon fibers for the thermal management of batteries has not been thoroughly investigated so far, and only a few studies have been conducted to increase the heat transfer coefficient of phase change materials in general. As a quick comparison, in previous studies, the range of increase in conduction heat transfer coefficient with randomized carbon fibers was between 85 and 130%, while in this study, by aligning carbon fibers radially, it rose by a factor of 8 to 13 times, compared to the base case.

THEORETICAL SECTION

The thermal performance of carbon fiber-loaded paraffin wax was numerically examined, while it is used as a thermal management medium for a Li-ion battery cell. A generic cylindrical Li-ion battery was allowed to dissipate constant heat rate, which in this case for a standard (*e.g.*, 14500 AA) Li-ion battery is equal to 2 W, (equivalent to 236.4 kW/m^3) into the cooling medium and the temperature distribution was obtained as a function of time.

In this research, COMSOL MutiPhysics was used for the modelings. The package is a powerful interactive

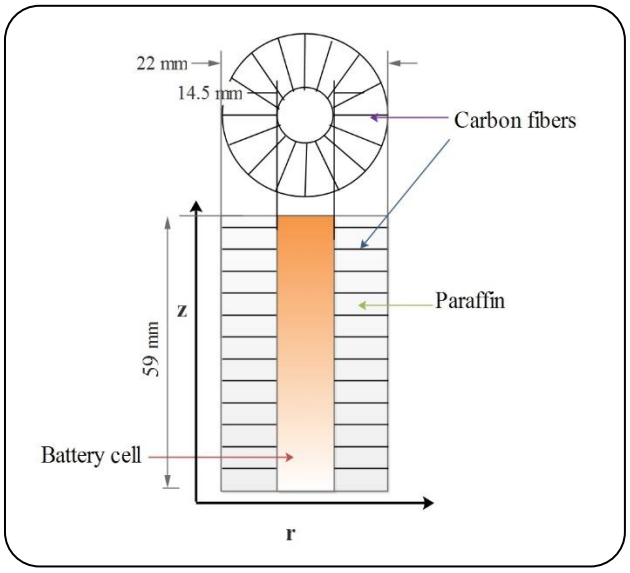

Fig. 1: The schematic diagram of the battery cell and the cooling system.

the software environment for modeling and solving various kinds of scientific and engineering problems. The software provides a powerful integrated desktop environment with a Model Builder that gives the user a full overview of the model with wide access to important functionalities.

Thermal management model

The schematic diagram of the cooling system is illustrated in Fig.1. As seen in this figure, a cylindrical battery is placed in the center of a rectangular container filled with coolant (*e.g.*, PCM composite). The heat generated inside the battery cell dissipates into the cooling medium, which can be either air, pure PCM (paraffin wax), or PCM loaded with carbon fibers, as shown in the figure. The composition and physical properties of paraffin and carbon fibers are given in Ref. [8]. As a result of heat transfer, the PCM is gradually heated, and if the heat transfer rate is sufficient, it melts down. The melting begins initially at the battery-PCM interface, and the melting zone extends toward the system boundaries as time elapses.

Governing equations

For the medium cooling under consideration, the governing equations for continuity, momentum, and energy are listed in Table 1 [38-39], where T_m is the medium cooling temperature, T_∞ is the ambient temperature, which is considered to be equal to 298.15 K, T_{ref} is a reference temperature (considered as 293.15 K),

Table 1: Governing equations.

Continuity equation	$\frac{\partial \rho}{\partial t}+\frac{1}{r}\frac{\partial}{\partial r}(\rho r u_r)+\frac{\partial}{\partial z}(\rho u_z)=0$	(1)
Equation of motion	$\rho\frac{\partial u}{\partial t}+\rho(u.\nabla)u=-\nabla P+\rho\vec{g}+\nabla.\bar{\tau}+\vec{F}$	(2)
Energy equation for the cooling medium (air, PCM, and carbon fiber-PCM composite)	$\rho c_p\frac{\partial T_m}{\partial t}+\rho c_p u.\nabla T_m=\nabla.(k\nabla T_m)$	(3)
Volume forces	$F_z=\rho g\beta(T-T_{ref})\quad F_r=0$	(4)
Initial conditions	At $t=0\quad T_m=298.15K$ $u_r=u_z=0\qquad P=\rho g(h_{batt}-z)$	(5)
Boundary conditions in fluid	At $r=R_{batt}:\ u_r=u_z=0$	(6)
Interfacial boundary conditions for battery and composite	$n.(q_1-q_2)=0$	(7)
Boundaries conditions at outer boundaries	$-n.(-k\nabla T_m)=h(T_\infty-T_m)$	
At the bottom of the battery and its enclosure	$\frac{\partial T}{\partial z}=0$	
The battery heat equation	$\rho_b c_{pb}\frac{\partial T_s}{\partial t}=Q$	(8)

Table 1: Correlations for thermo-physical properties of paraffin wax under melting conditions.

$k_{pcm}=\theta k_{phase1}+(1-\theta)k_{phase2}$	(9)
$(C_p)_{pcm}=\frac{1}{\rho}(\theta(C_p)_{phase1}+(1-\theta)(C_p)_{phase2})+L(\frac{\partial \alpha_m}{\partial T})$	(10)
$\alpha_m=\frac{1}{2}\frac{\theta\rho_{phase1}-(1-\theta)\rho_{phase2}}{\theta\rho_{phase1}+(1-\theta)\rho_{phase2}}$	(11)
$\rho_{pcm}=\theta\rho_{phase1}+(1-\theta)\rho_{phase2}$	(12)

Table 2: Thermo-physical properties of PCM composites.

$\rho_{comp}=\phi\rho_c+(1-\phi)\rho_{PCM}$		(15)
$c_{p,comp}=\frac{\phi(\rho C_p)_c+(1-\phi)(\rho C_p)_{PCM}}{\rho_{comp}}$		(16)
$L_{comp}=\frac{(1-\phi)(\rho L)_{PCM}}{\rho_{comp}}$		(17)
$\mu_{comp}=0.983e^{(12.959\phi)}\mu_{PCM}$		(18)
$k_{comp}=\phi k_c+(1-\phi)k_{PCM}$	Effective thermal conductivity (carbon fiber-PCM composite)	(19)

and T_s is the battery temperature. In these equations, g is the gravitational acceleration, β is the volumetric thermal expansion coefficient (1/K) and Q represents the rate of heat generation (per unit volume) within the battery, C_{pb} is the specific heat capacity, and ρ_b is battery density. C_p and ρ are respectively the paraffin heat capacity and density. Also, U_r is the fluid radial velocity, R_{batt} and h_{batt} are the battery radius and height, respectively. Thermal conductivity, specific heat, and density of the PCM are calculated based on correlations given in Table 2 [32, 38].

Where L denotes the latent heat of PCM and θ is the mass fraction of the liquid PCM. It is assumed that the PCM melting occurs between $T_{solidus}$ and $T_{liquidus}$.

Also, density, specific heat capacity, latent heat, and viscosity of the carbon fiber-loaded PCM composite are respectively defined in Table 3 [34-46].

Table 4: Simulation conditions.

Parameter	Symbols	Value	Comments
Fiber mass fraction [%]	W_0	0	Pure paraffin
	W_1	0.32	Radial and random
	W_2	0.46	Radial and random
	W_3	0.56	Radial and random
	W_4	0.69	Radial and random
Ambient temperature [K]	T_∞	298.15	-
Initial temperature [K]	T_0	298.15	Battery

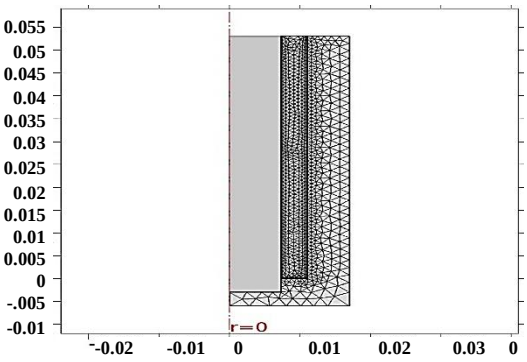

Fig. 2: Typical mesh grid used for numerical simulation.

Numerical solution

The mesh grid used for the numerical solution is shown in Fig. 2. The mesh is of a triangular, closed fan type for the box with sizes of 1.18×10^{-4} m (minimum) and 0.0059 m (maximum) with a curvature factor of 0.4. For the fluid around the battery (*i.e.*, melting paraffin), the minimum mesh size, the maximum mesh size, and the curvature factor are chosen to be 0.0014 m, 6.8×10^{-5} m, and 0.6, respectively. For the system boundaries, the mesh types are triangular shapes with the minimum mesh size, maximum mesh size, and curvature factor of 3.4×10^{-5}, 7.65×10^{-4} m, and 0.3, respectively.

A numerical solution technique based on the finite volume method is used to solve the governing equations. The solution scheme is implicit Backward Differentiation Formula (BDF) of maximum second order with a time step of 0.1 min. The resulting equations are solved by the Jacobi method.

RESULTS AND DISCUSSION

The thermal performance of a single cylindrical battery cell is studied during a constant rate of discharge while dissipating heat into ambient air or a PCM composite. Time variations of velocity, temperature, thermal conductivity, and thermo-physical properties are studied under various boundary conditions. The battery surface temperature (T_s) is computed as a function of time, but it is reported at the mid-height (z=0.028m). The simulation results obtained for different cooling media, including air (*i.e.*, natural convection), pure paraffin wax, and carbon fiber loaded (both randomly distributed and radially oriented) paraffin wax are presented and compared. In addition, effective thermal conductivity (k_m) is compared with those of pure paraffin. The total heat dissipation rate is set at 2 W for all simulation cases. Table 4 lists various conditions under which simulations were conducted.

Thermal behavior

Fig. 3 shows temperature profiles within the battery container at different time periods. The cooling medium is considered to be air, which naturally moves inside the container during the simulation. It is seen from the results that the surface temperature of the battery increases sharply from the initial value and reaches 70 °C (340 K) in 60 min. This temperature is much higher than the maximum allowable operating temperature for Li-ion batteries of 45-55 °C [10, 32].

The time variation of the battery (surface) temperature is shown in Fig. 4. As seen from this figure, the temperature monotonically increases with time. However, the rate of temperature change is maximum at the beginning. his rate diminishes as time passes, and the battery

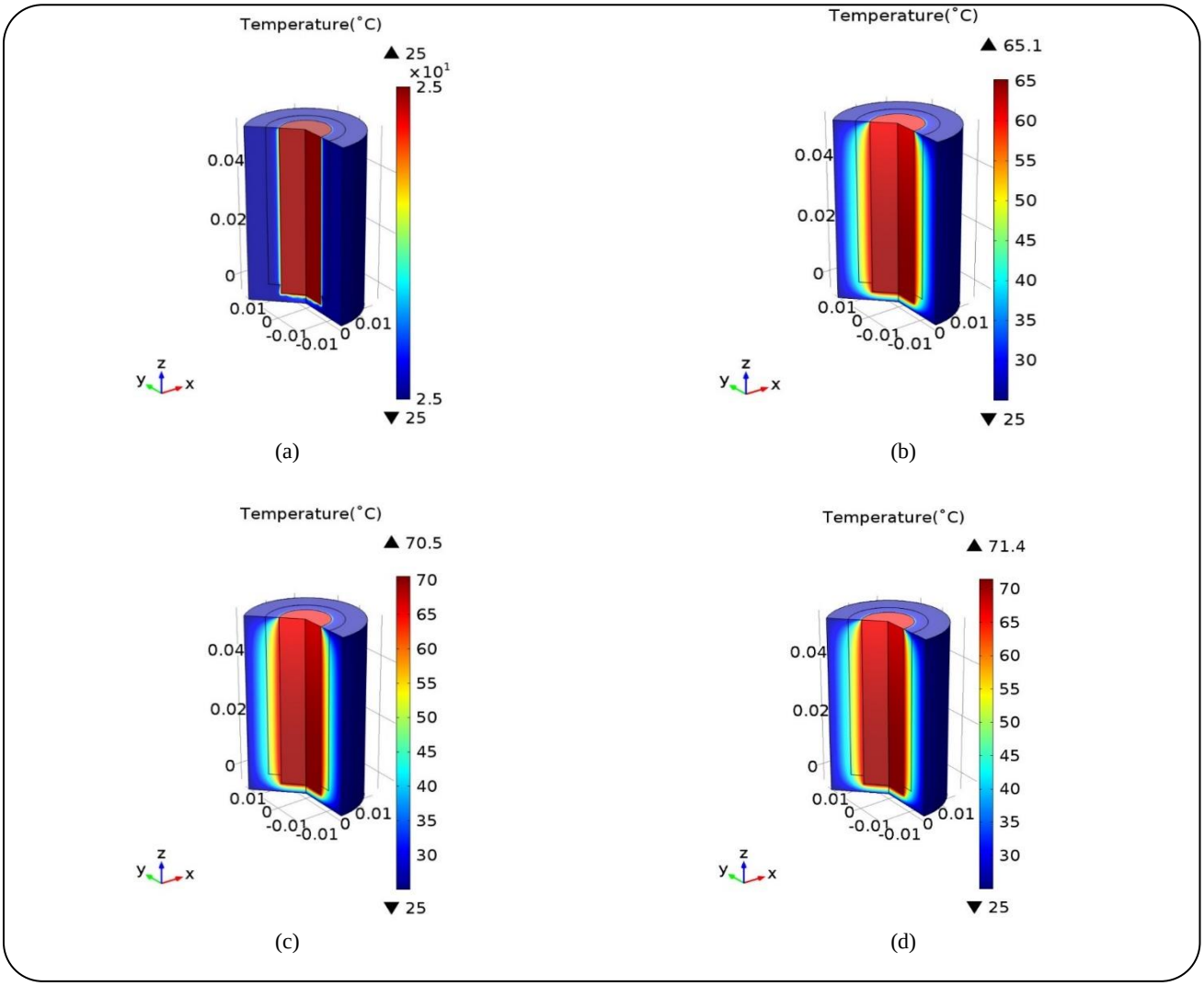

Fig. 2: Temperature profiles within the battery container for natural convection air cooling as a function of time, (a): t=0, (b): t=30, (c): t=60 and (d): t=90 min.

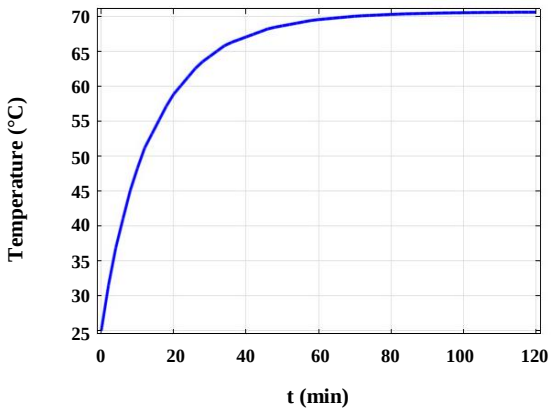

Fig. 3: Time variation of battery temperature for natural convection air cooling.

temperature approaches a constant value close to 70 °C (343 K) after 120 min of operation. The simulation results clearly show that naturally convecting air is not an effective cooling medium for the thermal management of such batteries.

Thermal behavior is dramatically improved if the cooling air is replaced with PCM, as displayed in Figs. 5 and 6. As can be seen from Fig. 6, the battery body temperature rises to 57.5 °C (330.5 K) after 120 min, which is much lower than the maximum temperature observed under natural convection air cooling. This temperature is within the appropriate design range suggested for Li-ion batteries. It must be noted that the sudden change in temperature slope after about 20 min. is due to the melting of PCM, which occurs at 45°C.

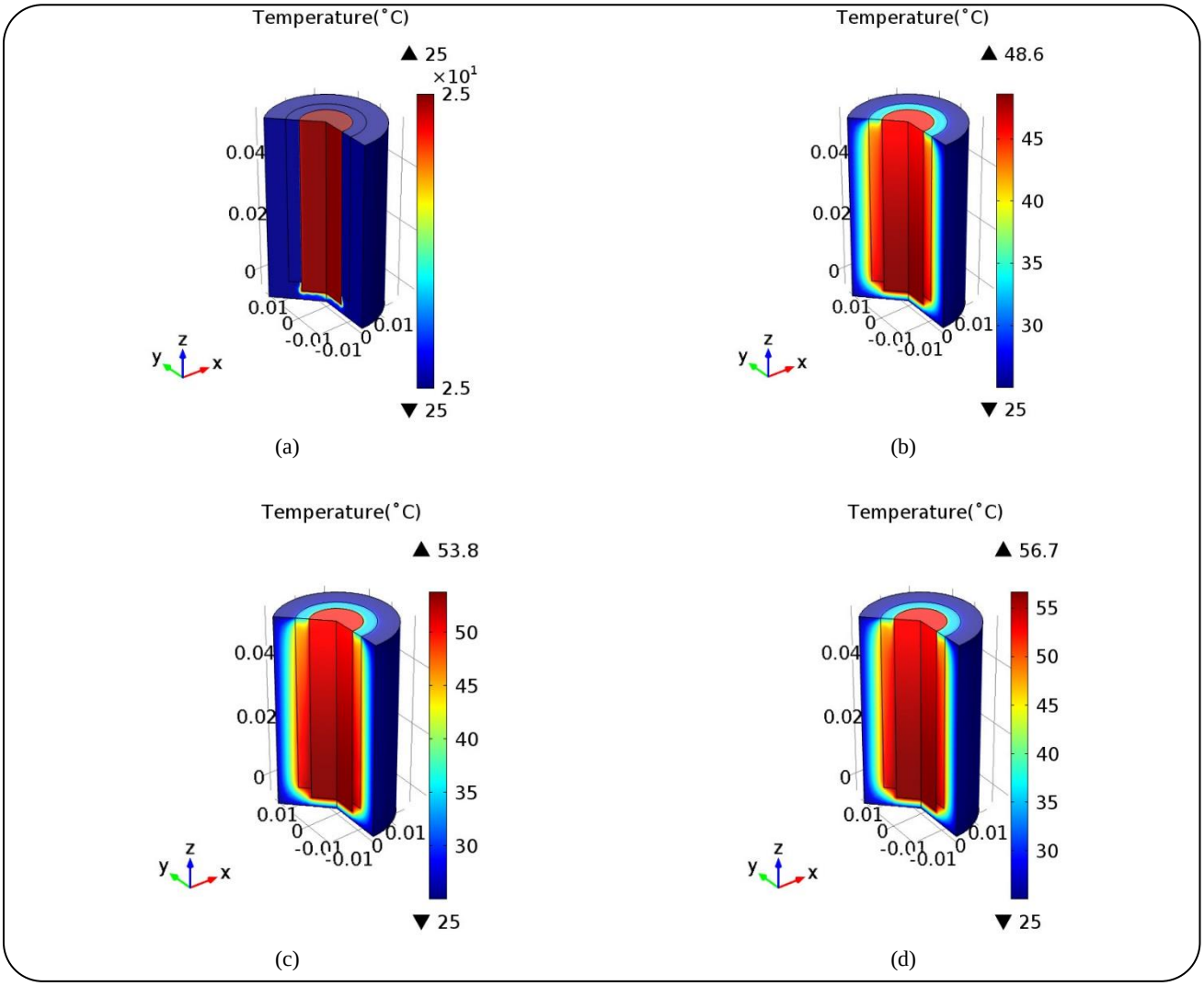

Fig. 4: Temperature profiles within the battery container when pure PCM is used as the cooling medium as a function of time, (a): t=0, (b): t=30, (c): t=60 and (d): t=90 (min).

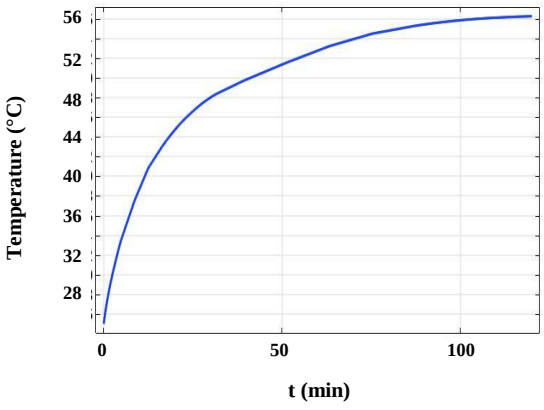

Fig. 6: Time variation of battery surface temperature when pure PCM is used as the cooling medium.

With a thermal conductivity of about 50 W/m K, the relatively low density and flexible carbon fibers are excellent thermal links to promote heat transfer in PCMs. However, it is expected that the pattern of carbon fiber distribution can influence the rate of heat transfer within the PCM. Fig. 7 depicts the three-dimensional temperature profiles in the coolant PCM loaded with 0.69 wt.% (sample W_4) carbon fibers, which are radially oriented within the coolant at different times. It is noteworthy that although Figs. 3 and 5 look similar, in fact, they are quite different as different heat transfer mechanisms affect the system. The difference can be highlighted by comparing Figs. 4 and 6, which depict the battery surface temperatures accordingly. However, in Fig. 7, with the presence of carbon fibers, there is a combination of heat transfer mechanisms, as conduction heat transfer through carbon fibers presents.

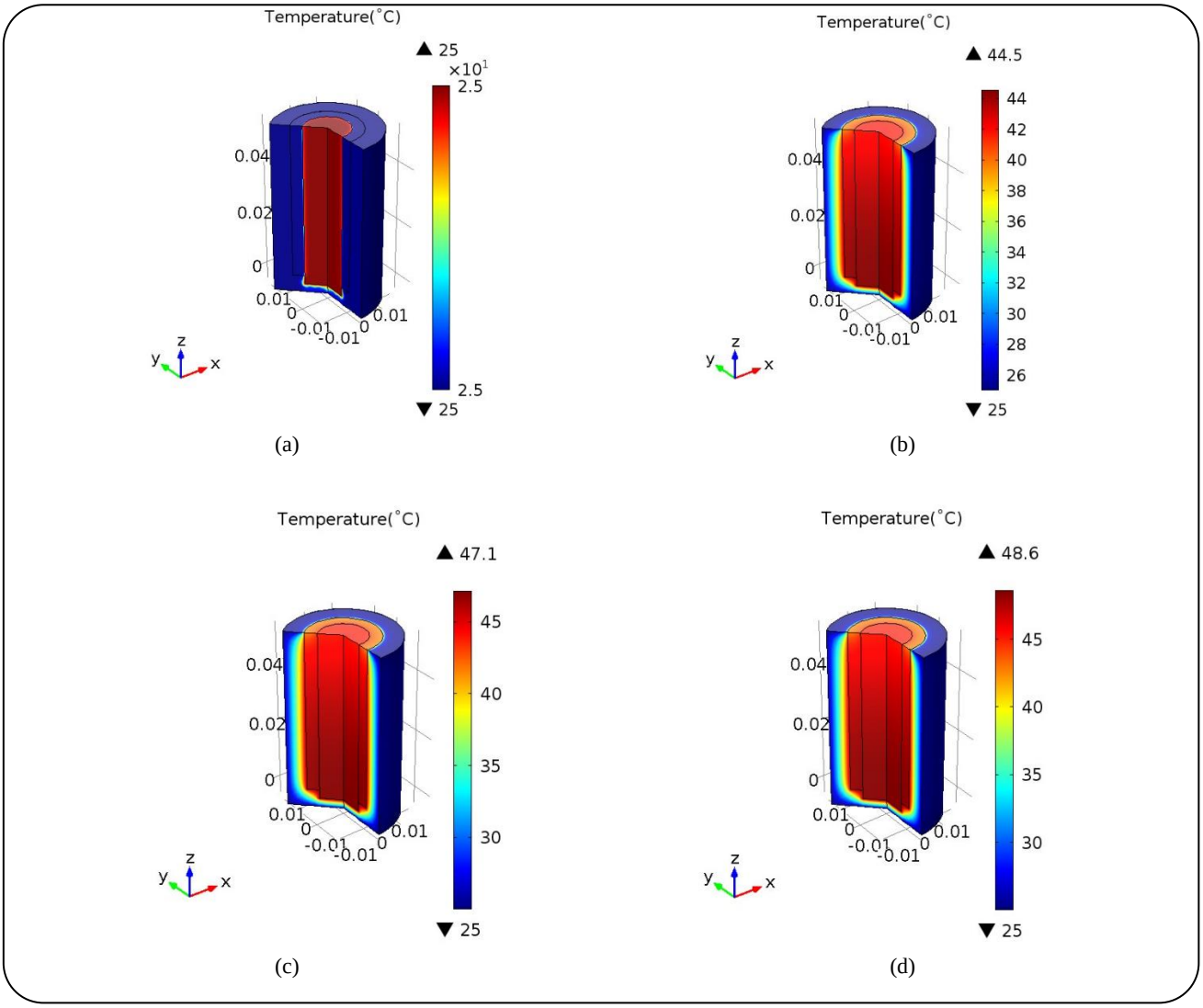

Fig.7: Temperature profiles within the battery container when PCM is loaded with radially distributed carbon fibers as a function of time, (a): t=0, (b): t=30, (c): t=60 and (d): t=90 (min).

Fig. 8 displays time variations of the battery surface temperature while dissipating heat into the carbon fiber composites (radial and random distributions) at different carbon fiber loadings. It is evident from the figure that the presence of carbon fibers improves the battery thermal management (6 °C lower at the end) when carbon fibers are uniformly (radially) distributed as compared to those of random distributions. The advantage of radial over random distributions is the constant, uniform, and non-agglomerating distribution of carbon fibers under which thermo-physical properties of carbon fibers are better realized in the composite medium.

Fig. 9 shows how the presence of carbon fibers (radial or random) in the PCM affects the temperature variations in the r-direction (z=53 mm) for different carbon fiber loadings. An extra temperature drop of about 6.5 °C (2.01%) in the maximum temperature is observed when carbon fibers are distributed radially throughout the PCM. A remarkable result is that the temperature difference between the battery surface and the container walls (maximum - minimum) is approximately 0.5 °C for radially distributed carbon fibers. This is a good indication that better thermal diffusion occurs when carbon fibers are orderly distributed in the PCM. The lower thermal diffusivity of the random arrangement can be attributed to several reasons, including the agglomeration of fibers.

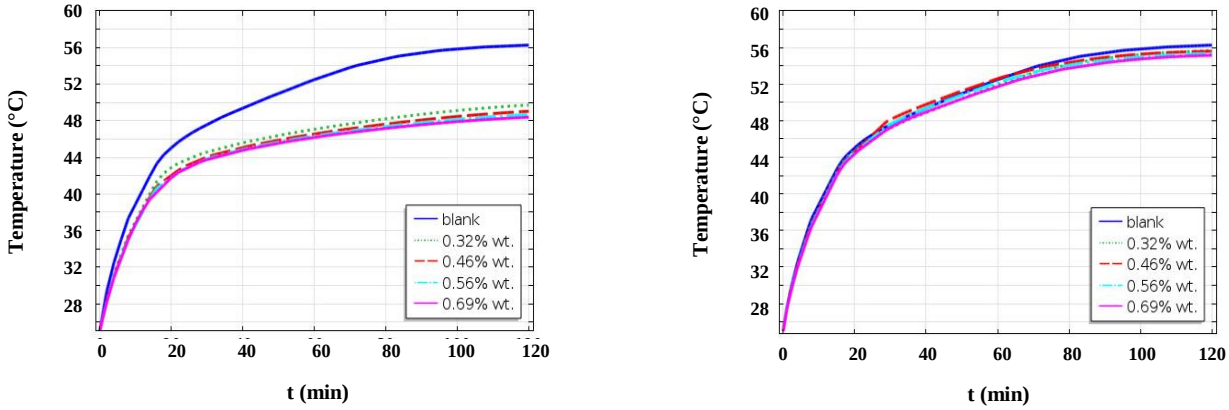

Fig. 8: Time variation of the battery surface temperature for various carbon fiber loaded PCMs as the cooling medium, (a) radial distribution and (b) random distribution.

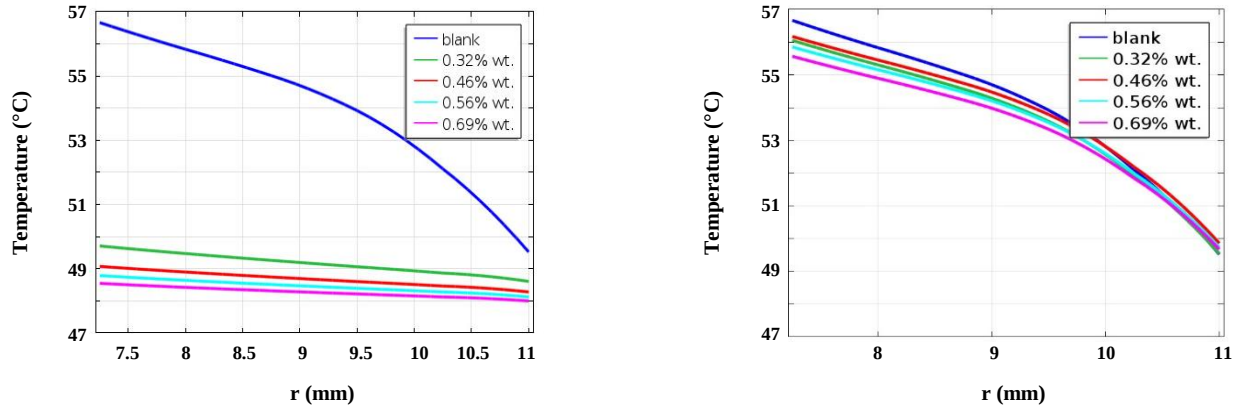

Fig. 9: Steady-state temperature profiles in r-direction for various carbon fiber loadings (a) radial distribution and (b) random distribution.

From the simulation results, one can conclude that the presence of carbon fibers in a PCM (both mass fraction and the pattern of distribution) has a significant effect on the battery performance.

Velocity distribution

The generated heat from the discharging battery transfers into the cooling medium and can cause fluid circulation inside the container. Figs. 10.a and b show the velocity distributions for the coolant air at 30 and 90 min after the battery starts discharging. As expected, the air is heated initially at the battery surface and moves upward along the battery. Since the container is assumed to be enclosed, the heated air changes direction at the top and moves downward along the container walls. The air circulation is enhanced as more heat is dissipated from the battery. A maximum velocity of about 8 mm/s is predicted after 90 min of battery operations.

Figs. 10.c and d show the velocity distributions in the PCM without carbon fibers (blank PCM) after 30 and 90 min. As time elapses, the PCM heats up, and if the temperature exceeds the melting point, a phase change occurs, and the liquefied paraffin wax circulates within the container. However, compared to the coolant air, it is harder for the liquefied PCM to circulate around the battery, and as a result, smaller velocities are obtained. Figs. 10.e and f depict velocity distributions for PCM loaded with radially distributed carbon fibers (0.69 wt. %). This time, the velocity of molten paraffin is smaller than that of the pure paraffin wax because the radially fixed fibers impede the free motion of molten paraffin. It is also seen that in the first 30 min of the simulations, just about

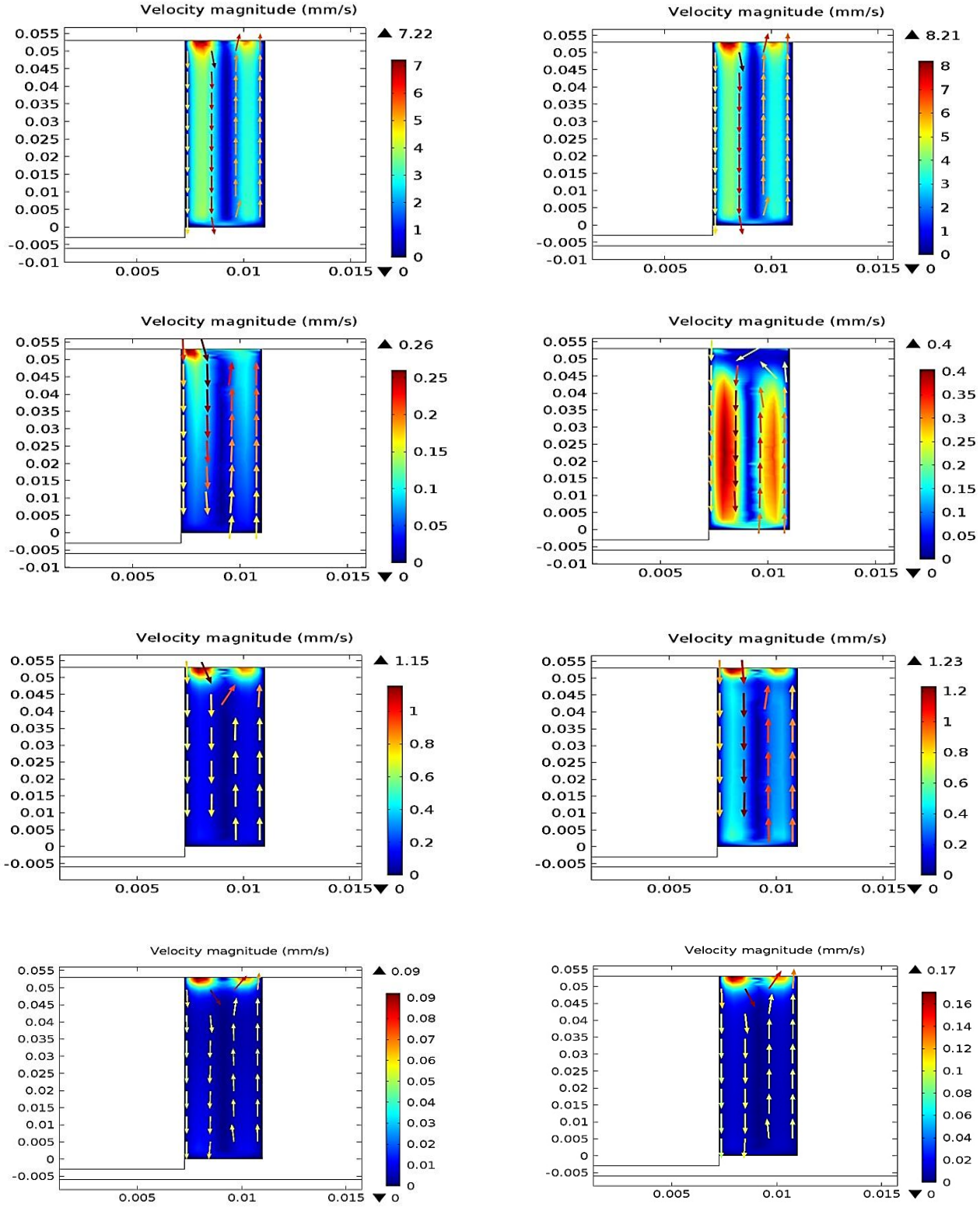

Fig. 10: Velocity distributions in various cooling media (a) air at t=30 min (b) air at t=90 (min) (c) blank PCM at t=30 min (d) blank PCM at t=90 (min), (e)random fiber arrangement at t=30 and (f) random fiber arrangement at t=90 (min) (g) radial arrangement, (W_4) at t=30 and (h) radial arrangement, (W_4) at t=90 (min).

15% of the paraffin is melted, and most of the medium is still in solid form. This is the reason for observing an increased velocity in this period.

Thermal conductivity enhancement

One of the main drawbacks of PCMs in energy storage applications is their low thermal conductivities. The effective thermal conductivity (or thermal diffusivity) can be improved by adding highly conductive materials such as carbon fibers into the PCM. Compared to the traditional heat transfer promoters such as metal oxide nanoparticles, carbon fibers offer a relatively higher thermal conductivity (about 50 W/m K) and low density at a reasonable price. The effective thermal conductivity of carbon fiber-loaded PCM (k_{eff}) can be expressed according to Fourier law of heat conduction.

$$q = -k_{eff} \nabla T \tag{21}$$

Using the battery heat dissipation rate, and the calculated temperature profiles, the effective thermal conductivity of the PCM composites is determined. Fig. 11 shows variations of the mean effective thermal conductivity in the radial direction based on the values along the battery length for pure paraffin at different times. In the early stages of the operation (*e.g.*, 30 min), only a portion of the paraffin (near the battery) is melted and since the thermal conductivity of molten paraffin is lower than that of the solid form (0.21 W/m K for solid paraffin, and 0.12 W/m K for liquid paraffin), smaller thermal conductivities are observed in this region. As time passes by, more PCM is liquefied, and as a result, smaller constant thermal conductivities are obtained [47-50]. Numerical results in Fig. 11 show that similar thermal conductivities prevail in the r-direction after 90 min of battery operation.

Fig. 12 shows the variation of the mean thermal conductivity of different PCM composites in the radial direction as a function of time. It is seen that with the presence of carbon fibers, the trend of variation changes. The presence of carbon fibers with thermal conductivity of k=50W/m K in the PCM has caused more uniform temperature profiles in the radial direction because of the improved thermal conductivities. Consequently, the slopes of the variations of mean effective thermal conductivity decreased.

Knowing the thermal conductivity of pure PCM, a thermal conductivity enhancement factor (η), can be defined as [7, 14]:

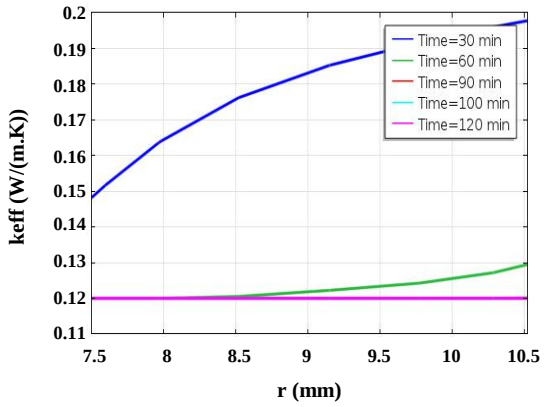

Fig. 11: Variation of the mean thermal conductivity of pure paraffin versus time.

$$\eta = \frac{k_{eff,c} - k_{eff,b}}{k_{eff,b}} \tag{22}$$

Where $k_{eff,c,}$ and $k_{eff,b}$ denote effective thermal conductivity of the composite and carbon-fiber free PCM (blank), respectively.

Fig. 13 shows the simulation results for the thermal conductivity enhancement factor of PCM composites versus time for the radially oriented carbon fibers, and Fig. 14 depicts the same parameter for the random arrangement.

According to the definition given in Eq. (22), the enhancement factor (η) for a fiber-free PCM (blank) is zero. The presence of carbon fibers in the PCM considerably improves the effective thermal conductivity considerably. However, this parameter depends on the mass fraction of the carbon fibers used as well. In addition, PCMs with higher carbon fiber loadings (*e.g.*, W_3 and W_4) have a steadier trend, and their thermal conductivity enhancement factors remain approximately constant. On the other hand, samples with smaller carbon fiber loadings (W_1 and W_2) show unsteady performance owing to the small and unsteady variation of temperature difference (not temperature) of these samples. In other words, samples containing small amounts of carbon fibers have a performance similar to the blank, and that is why the thermal conductivity enhancement factor of these samples is unsteady [32].

There are several essential points that can be inferred from Figs. 13 and 14 concerning the thermal conductivity enhancement factor. First, η is much higher for the radial arrangement (almost ten times) than that of the random arrangement. Second and more importantly, the radial

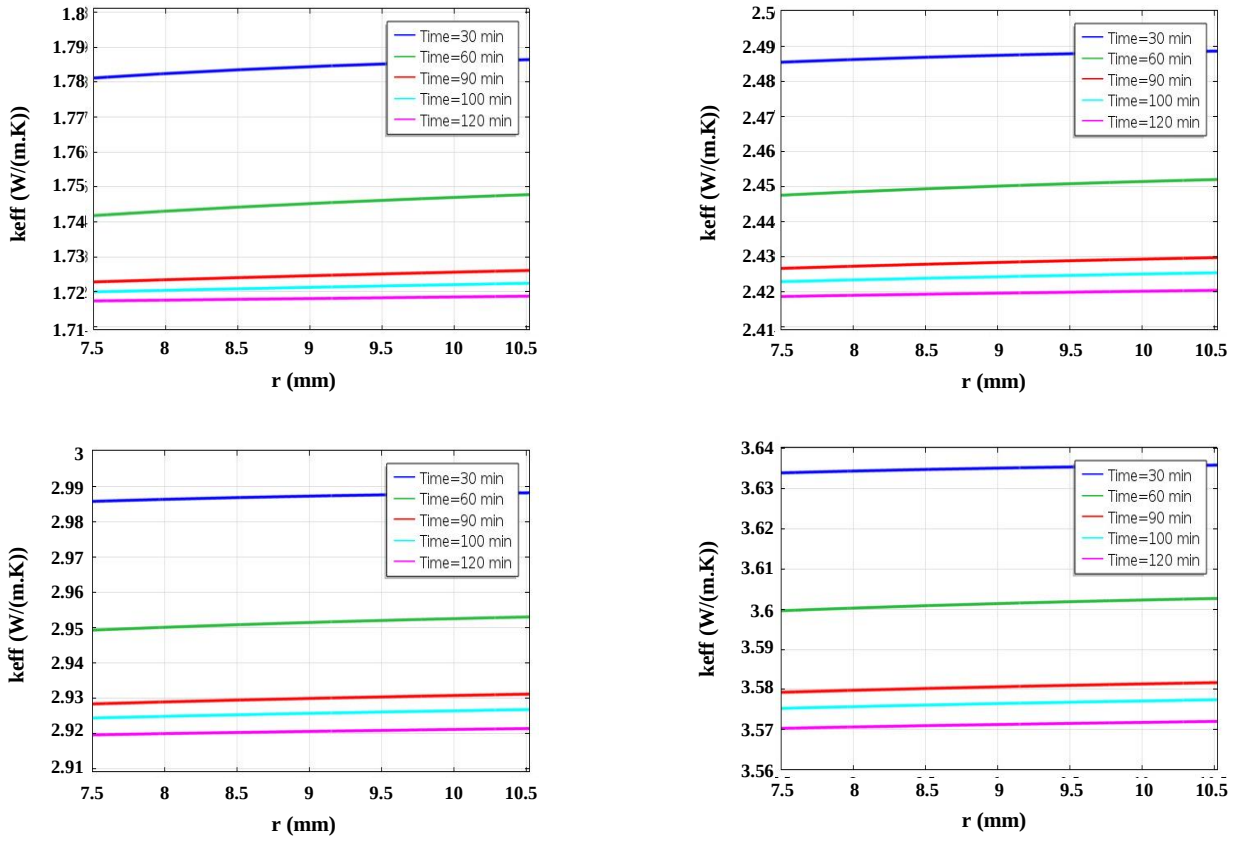

Fig. 12: Variation of the mean thermal conductivity of different PCM composites in radial direction versus time, (a) W_1, (b) W_2, (c) W_3 and (d) W_4 (radial arrangement).

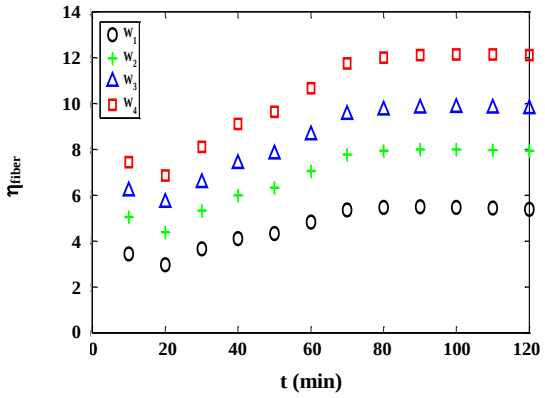

Fig. 13: Thermal conductivity enhancement factor of the PCM composites with radially oriented carbon fibers.

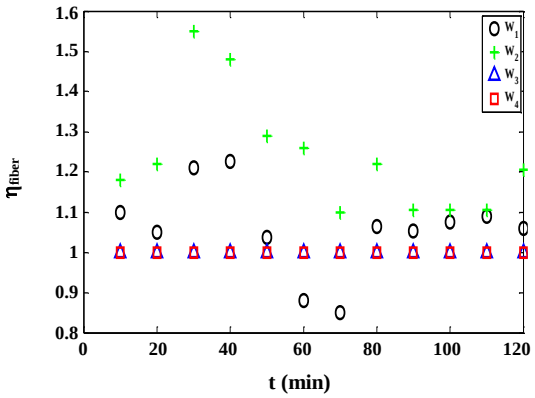

Fig. 14: Thermal conductivity enhancement factor of the PCM composites with randomly distributed carbon fibers

the arrangement, η follows an orderly pattern at different times, while for the random arrangement, a changing trend is observed. Also, as the weight fraction of carbon fibers increases (for radially arranged carbon fibers), η increases in an almost orderly manner, while for random distribution, no clear pattern can be observed. The radial arrangement is a better choice for battery thermal management systems in all aspects.

Phase change state

The state of phase change for PCM/composite is very crucial during energy storage (or retrieval) since it has

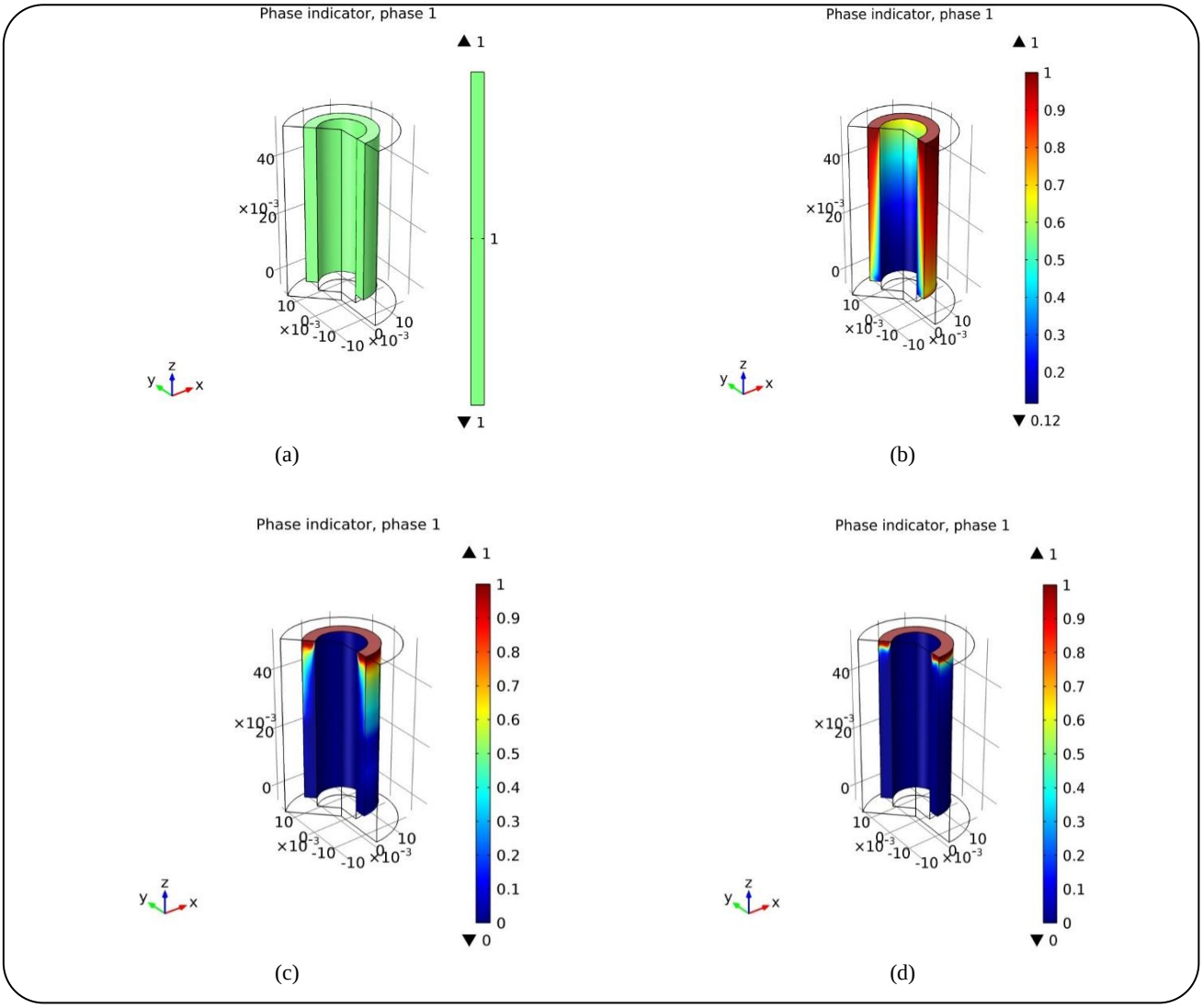

Fig. 15: Phase transition in pure paraffin (W0), (a) t=0, (b) t=30, (c) t=60, (d) t=90 min (phase 1 is the solid phase).

direct influence on the viscosity, velocity distribution, and the resulting temperature profile. In this section, the phase conditions for the pure paraffin and composite samples are presented and compared. As can be seen in Figs. 15 to 17, when the battery discharges, the melting starts at the battery surface and moves radially away towards the boundary for both PCM and PCM composite. However, compared to pure paraffin, the phase transition is slightly slower than that of the composite with radial or random carbon fiber distributions [51-53].

As mentioned before, the presence of carbon fibers in PCM promotes heat transfer from the battery with better heat transfer in paraffin, first, the battery temperature is maintained at lower values and second, more heat reaches the points near the outer walls and hence better heat dissipation to the environment is achieved. Consequently, the average temperature within the entire system (the battery and cooling medium) is reduced, which results in a lesser phase change in the composite. In other words, in such conditions, the addition of carbon fibers results in more uniform temperature distribution and phase change in the composite. It is worthy of the attention that these effects are more profound in the case of the radial distribution of carbon fibers.

CONCLUSIONS

Phase change materials are considered an essential part of advanced thermal management systems. They have

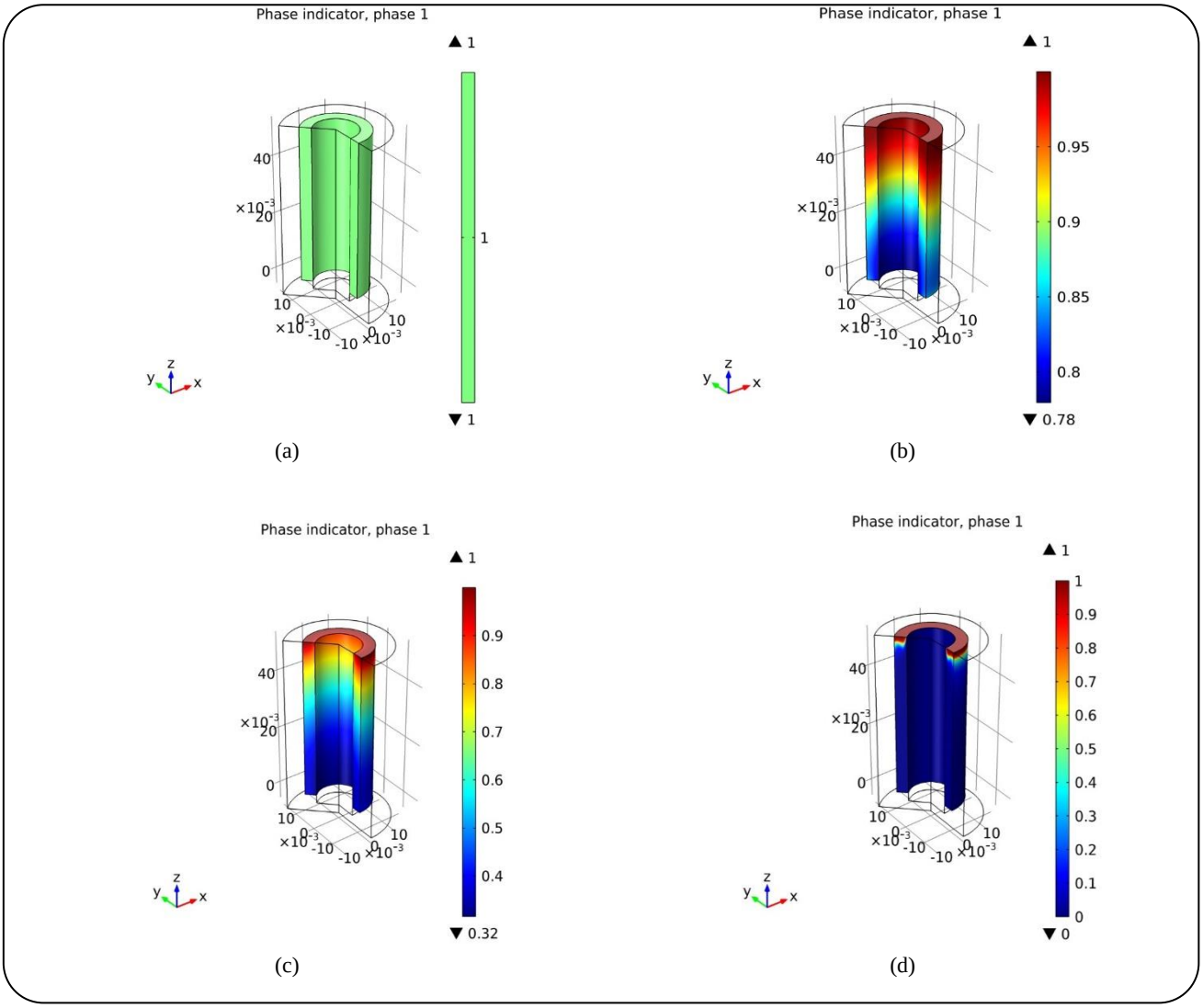

Fig. 16: Phase transition in PCM composite (W4, radial arrangement), (a): t=0, (b): t=30, (c): t=60 and (d): t=90 min (phase 1 is the solid phase).

the potential to prevent overheating of sensitive electronics, instruments, and appliances. In this study, the thermal behavior of a typical Li-ion battery cell was simulated numerically in the presence of carbon fiber-loaded paraffin wax (as PCM). Two different arrangements were considered for the carbon fibers: radial and random distributions. It was identified that the air is certainly an inefficient cooling medium for the thermal management of the Li-ion battery under investigation, while PCM alone can mark an improvement in thermal performance in comparison to the air. It was observed that the PCM composite with radially arranged carbon fibers exhibits much better thermal performance than the PCM composite with randomly distributed carbon fibers. The temperature difference between the battery surface and the container walls (maximum-minimum) were found to be approximately 0.5 °C for radially distributed carbon fibers. Also, the results showed that a ten-fold increase in thermal conductivity enhancement can be achieved when carbon fibers are distributed in the radial direction as compared with random distribution. As a matching combination, radially-distributed carbon fibers shortcut the thermal resistance, while the PCM provides heating/cooling capacity. Application of carbon fiber and phase change materials for thermal management of future batteries maybe associated with complexities such as orderly dispersion maybe of carbon fibers and may not be cost-effective. To solve these problems, one can use carbon fiber brushes

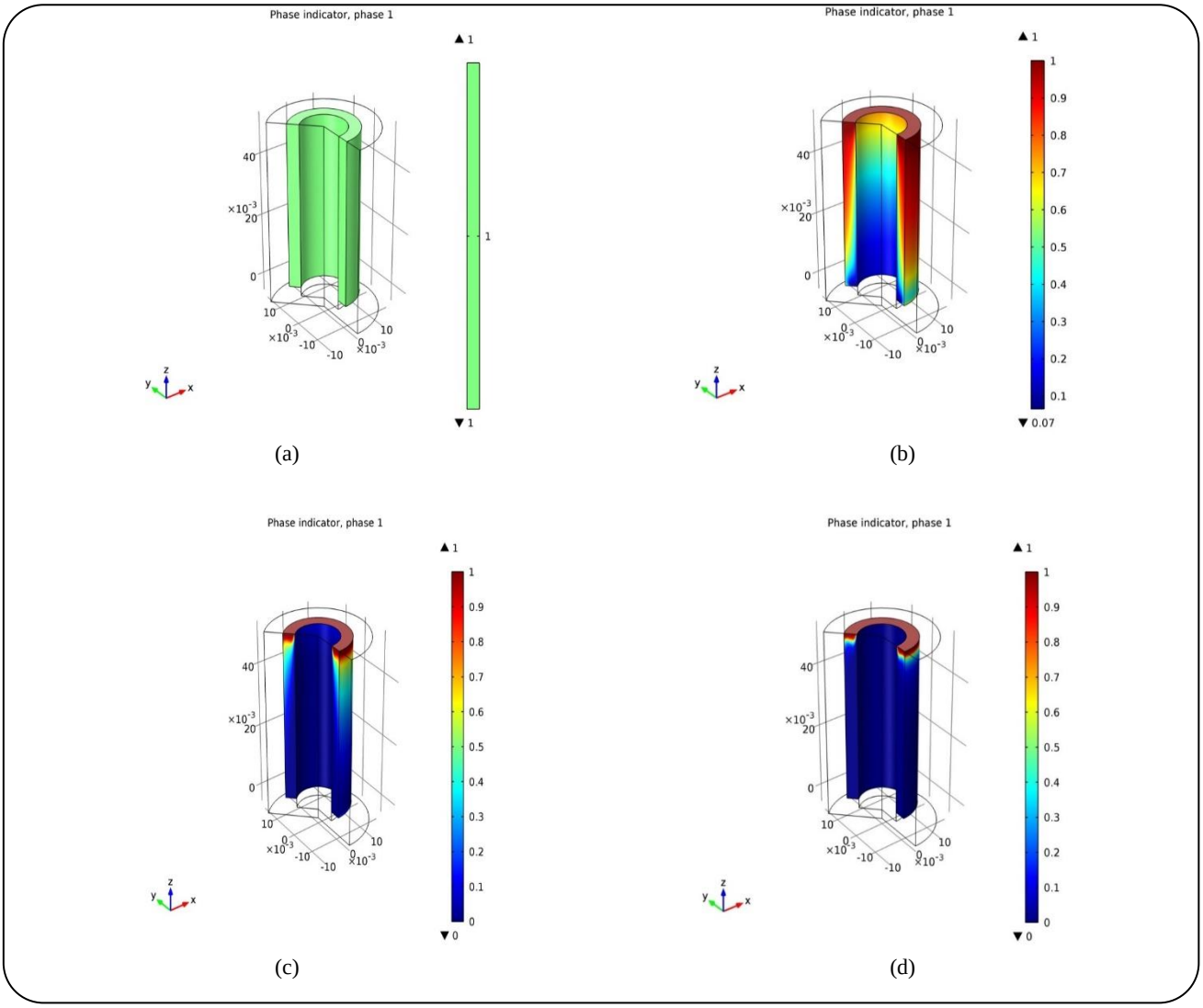

Fig. 17: Phase transition for PCM composite (W4, random arrangement), (a) t=0, (b) t=30, (c) t=60 and (d) t=90 min (phase 1 is the solid phase).

as a set or increase the amount of carbon fiber in the composite to reduce the total volume of the system.

Nomenclature

C_p	Specific heat capacity, J/mol K
F	Volume force, N/m^3
G	Acceleration of gravity, m/s^2
H	Heat transfer coefficient, W/m^2 K
L	Latent heat of the PCM, J/kg
K	Thermal conductivity, W/m K
P	Pressure, Pa
ΔP	pressure changes, Pa
Q	Volumetric heat source, W/m^3
r	Radial distance, mm
T	Temperature, °C /K
t	Time, s
U	Radial velocity components, m/s
W	Carbon fiber mass fraction
Z	Axial distance, mm

Greek letters

β	Volumetric thermal expansion coefficient, 1/K
η	Thermal conductivity enhancement factor
Θ	Liquid fraction
μ	Viscosity, Pa. s
ρ	Density, kg/m^3
τ	Shear stress, Pa

φ	Carbon fiber mass fraction

Superscripts and subscripts

b	Blank
batt	Battery
c	Carbon fiber
comp	Carbon fiber-PCM composite
eff	Effectively
ref	Reference state

Abbreviations

CFD	Computational fluid dynamic
Li-ion	Lithium-ion
PCM	Phase change material

Received : Jon. 6, 2020 ; Accepted : Oct. 12, 2020

REFERENCES

[1] Goli P., Legedza S., Dhar A., Salgado R., Renteria J., Balandin A. A., Graphene-enhanced Hybrid Phase Change Materials for Thermal Management of Li-Ion Batteries, *J. Power Sources*, **248**: 37-43 (2014).

[2] Duan X., Naterer G. F., Heat Transfer in Phase Change Materials for Thermal Management of Electric Vehicle Battery Modules, *Int. J. Heat Mass Transfer*, **53(23-24)**: 5176–5182 (2010).

[3] Ramandi M. Y., Dincer I., Naterer G. F., Heat Transfer and Thermal Management of Electric Vehicle Batteries with Phase Change Materials, *J. Heat Mass Transfer*, **47(7)**: 777-788 (2011).

[4] Zalba B., Marıń J. M., Cabeza L. F., Mehling H., Review on Thermal Energy Storage with Phase Change: Materials, Heat Transfer Analysis and Applications, *Appl. Therm. Eng.*, **23(3)**: 251–83 (2003).

[5] Najafi B., Bahari M., Babapoor A., Evaluation of α-AL_2O_3-PW Nanocomposites for Thermal Energy Storage in the Agro-products Solar Dryer, *J. Energy Storage*, **28**: 101181 (2020).

[6] Sakkaki M., Sadegh Moghanlou F., Parvizi S., Baghbanijavid H., Babapoor A., Shahedi Asl M., Phase Change Materials as Quenching Media for Heat Treatment of 42CrMo4 Steels, *J. Central South University*, **27**: 752-761 (2020).

[7] Xia L., Zhang P., Wang R. Z., Preparation and Thermal Characterization of Expanded Graphite/Paraffin Composite Phase Change Material, *Carbon*, **48(9)**: 2538-2548 (2010).

[8] Babapoor A., Azizi M., Karimi G., Thermal Management of a Li-Ion Battery Using Carbon Fiber-PCM Composites, *Appl. Therm. Eng.*, **82**: 281-90 (2015).

[9] Babapoor A., Karimi G., Khorram M., Fabrication and Characterization of Nanofiber-Nanoparticle-Composites with Phase Change Materials by Electrospinning, *Appl. Therm. Eng.*, **99**: 1225–1235 (2016).

[10] Babapoor A., Karimi G., Thermal Properties Measurement and Heat Storage Analysis of Paraffin-nanoparticles Composites Phase Change Material: Comparison and Optimization, *Appl. Therm. Eng.*, **90**: 945-951 (2015).

[11] Wang Z., Li X., Zhang G., Lv Y., Wang C., He F., Yang C., Yang Ch., Thermal Management Investigation for Lithium-ion Battery Module with Different Phase Change Materials, *RSC Adv.*, **7(68)**: 42909-42918 (2017).

[12] Maxa J., Novikov A., Nowottnick M., Thermal Peak Management Using Organic Phase Change Materials for Latent Heat Storage in Electronic Applications, *Materials*, **11**: 31-45 (2018).

[13] Babapoor A., Karimi G., Sabbaghi S., Thermal Characteristic of Nanocomposite Phase Change Materials During Solidification Process, *J. Energy Storage*, **7**: 74-81 (2016).

[14] Karimi G., Azizi M. M., Babapoor A., Experimental Study of a Cylindrical Lithium-ion Battery Thermal Management Using Phase Change Material Composites, *J. Energy Storage*, **8**: 168–174 (2016).

[15] Babapoor A., Karimi G., Golestaneh S. I., Ahmadi Mezjin M., Coaxial Electro-spun PEG/PA6 Composite Fibers: Fabrication and Characterization, *Appl. Therm. Eng.*, **118**: 398-407 (2017).

[16] Golestaneh S. I., Karimi G., Babapoor A., Torabi F., Thermal Performance of Co-electrospun Fatty Acid Nanofiber Composites in the Presence of Nanoparticles, *App. Energy*, **212**: 552-564 (2018).

[17] Usman H., Ali H. M., Arshad A., Ashraf M. J., Khushnood S., Janjua M., Kazi S. N., An Experimental Study of PCM Based Finned and Un-Finned Heat Sinks for Passive Cooling of Electronics, *Heat Mass Transfer*, **54**: 3587-3598 (2018).

[18] Fattahi M., Delbari S. A., Babapoor A., Sabahi Namini A., Mohammadi M., Shahedi Asl M., Triplet Carbide Composites of TiC, WC, and SiC, *Ceram. Int.*, **46(7)**: 9070-9078 (2020).

[19] Sabahi Namini A., Ahmadi Z., Babapoor A., Shokouhimehr M., Shahedi Asl M., Microstructure and Thermomechanical Characteristics of Spark Plasma Sintered TiC Ceramics Doped with Nano-Sized WC, *Ceram. Int.*, **45(2)**: 2153-2160 (2019).

[20] Fattahi M., Babapoor A., Delbari S. A., Ahmadi Z., Sabahi Namini A., Shahedi Asl M., Strengthening of TiC Ceramics Sintered by Spark Plasma via Nano-graphite Addition, *Ceram. Int.*, **46(8)**: 12400-12408 (2020).

[21] Barhemmati-Rajab N., Zhao W., Investigation into Boron Nitride Nanoparticle Effects on Thermal Properties of Calcium Chloride Hexahydrate ($CaCl_2 \cdot 6H_2O$) as a Phase Change Material, *MRS Commun.*, **8(4)**: 1439-1444 (2018).

[22] Babapoor A., Shahedi Asl M., Ahmadi Z., Sabahi Namini A., Effects of Spark Plasma Sintering Temperature on Densification, Hardness and Thermal Conductivity of Titanium Carbide, *Ceram. Int.*, **44(12)**: 14541-14546 (2018).

[23] Nguyen T. P., Shokouhimehr M., Azizian-Kalandaragh Y., Babapoor A., Van Le Q., Sabahi Namini A., Shahedi Asl M., Delbari S. A., Characteristics of Quadruplet Ti–Mo–TiB_2–TiC Composites Prepared by Spark Plasma Sintering, *Ceram. Int.*, (2020).

[24] Nguyen T. P., Pazhouhanfar Y., Delbari S. A., Sabahi Namini A., Babapoor A., Mohammadpour Derakhshi Y., Shaddel S., Van Le Q., Shokouhimehr M., Shahedi Asl M., Physical, Mechanical and Microstructural Characterization of TiC–ZrN Ceramics, *Ceram. Int.* (2020).

[25] Shahedi Asl M., Ahmadi Z., Sabahi Namini A., Babapoor A., Motallebzadeh A., Spark Plasma Sintering of TiC–SiCw Ceramics, *Ceram. Int.*, **45(16)**: 19808-19821 (2019).

[26] Al-Hallaj S., Kizilel R., Lateef A., Sabbah R., Farid M., Selman J. R., Passive Thermal Management Using Phase Change Material (PCM) for EV and HEV Li-ion Batteries, in: "*Vehicle Power and Propulsion IEEE Conference"* (2005).

[27] Khateeb S. A., Amiruddin S., Farid M., Selman J. R., Al-Hallaj S., Thermal Management of Li-ion Battery with Phase Change Material for Electric Scooters: Experimental Validation, *J. Power Sources*, **142(1-2)**: 345-353 (2005).

[28] Fukai J., Kanou M., Kodama Y., Miyatake O., Thermal Conductivity Enhancement of Energy Storage Media Using Carbon Fibers, *Energy Convers. Manage.*, **41(14)**:1543-1556 (2000).

[29] Haghighi A., Babapoor A., Azizi M. M., Javanshir Z., Ghasemzadeh H., Optimization of the Thermal Performance of PCM Nanocomposites, *J. Energy Manage. Technol.* (JEMT), **4(2)**: 14-19 (2020).

[30] Cao M., Huang J., Liu Z., The Enhanced Performance of Phase Change Materials via 3D Printing with Prickly Aluminum Honeycomb for Thermal Management of Ternary Lithium Batteries, *Adv. Mater. Sci. Eng.*, **2020**: (2020).

[31] Frusteri F., Leonardi V., Vasta S., Restuccia G., Thermal Conductivity Measurement of a PCM Based Storage System Containing Carbon Fibers, *Appl. Therm. Eng.*, **25(11-12)**: 1623-1633 (2005).

[32] Samimi F., Babapoor A., Azizi M. M., Karimi G., Thermal Management Analysis of a Li-ion Battery Cell Using Phase Change Material Loaded with Carbon Fibers, *Energy*, **96**: 355-371 (2016).

[33] Karimi G., Li X., Thermal Management of Lithium-ion Batteries for Electric Vehicles, *Int. J. Energy Res.*, **37(1)**:13-24 (2013).

[34] Karimi G., Dehghan Bidokhti A., Thermal Analysis of High-power Lithium-ion Battery Packs Using Flow Network Approach, *Int. J. Energy Res.*, **38**: 1793-811 (2014).

[35] Karimi G., Dehghan Bidokhti A., Thermal Management Analysis of a Lithium-ion Battery Pack Using Flow Network Approach, *Int. J. Mech.*, **1**: 188-194 (2102).

[36] Al-Hallaj S., Selman J. R., Thermal Modeling of Secondary Lithium Batteries for Electric Vehicle/Hybrid Electric Vehicle Applications, *J. Power Sources*, **110(2)**: 341-348 (2002).

[37] Javani N., Dincer I., Naterer G. F., Numerical Modeling of Submodule Heat Transfer with Phase Change Material for Thermal Management of Electric Vehicle Battery Packs, *J. Therm. Sci. Eng. Appl.*, **7(3)**:031005 (2015).

[38] Valan Arasu A., Mujumdar A. S., Numerical Study on Melting of Paraffin Wax with Al_2O_3 in a Square Enclosure, *Int. Commun. Heat Mass Transfer*, **39(1)**:16-22 (2012).

[39] Patankar S. V., "Numerical Heat Transfer and Fluid Flow (Series in Computation and Physical Processes in Mechanics and Thermal Sciences)", Hemisphere Publishing Company (1980).

[40] Chow L. C., Zhong J. K., Thermal Conductivity Enhancement for Phase Change Storage Media, *Int. Commun. Heat Mass Transfer*, **23(1)**:91-100 (1996).

[41] Vajjha R. S., Das D. K., Namburu P. K., Numerical Study of Fluid Dynamic and Heat Transfer Performance of Al_2O_3 and CuO Nanofluids in the Flat Tubes of a Radiator, *Int. J. Heat Fluid Flow*, **31(4)**: 613-621 (2010).

[42] Kandasamy R., Wang X. Q., Mujumdar A. S., Transient Cooling of Electronics Using Phase Change Material (PCM)-Based Heat Sinks, *Appl. Therm. Eng.*, **28(8-9)**: 1047–1057 (2008).

[43] Sasmito A. P., Kurnia J. C., Mujumdar A. S., Numerical Evaluation of Laminar Heat Transfer Enhancement in Nanofluid Flow in Coiled Square Tubes, *Nanoscale Res. Lett.*, **6(1)**: 376-90 (2011).

[44] Rao Y., Frank D., Peter S., Convective Heat Transfer Characteristics of Microencapsulated Phase Change Material Suspensions in Mini-channels, *Heat Mass Transfer*, **44(2)**:175-186 (2007).

[45] Sabbah R., Farid M. M., Al-Hallaj S., Micro-channel Heat Sink with Slurry of Water with Microencapsulated Phase Change Material: 3D-numerical Study, *Appl. Therm. Eng.*, **29(2-3)**: 445-454 (2009).

[46] Fukai J., Hamada Y., Morozumi Y., Miyatake O., Effect of Carbon-fiber Brushes on Conductive Heat Transfer in Phase Change Materials, *Int. J. Heat Mass Transfer*, **45(24)**:4781-4792 (2002).

[47] Valan Arasu A., Sasmito A. P., Mujumdar A. S., Numerical Performance Study of Paraffin Wax Dispersed with Alumina in a Concentric Pipe Latent Heat Storage System, *Therm. Sci.*, **17(2)**: 419-430 (2013).

[48] Mohammadi Khoshraj B., Seyyed Najafi F., Mohammadi Khoshraj J., Ranjbar H., Microencapsulation of Butyl Palmitate in Polystyrene-co-Methyl Methacrylate Shell for Thermal Energy Storage Application, *Iran. J. Chem. Chem. Eng.* (IJCCE), **37(3)**: 187-194 (2018).

[49] Li J., Effect of Fiber Surface Treatment on Wear Characteristics of Carbon Fiber Reinforced Polyamide 6 Composites, *Iran. J. Chem. Chem. Eng. (IJCCE)*, **29(1)**: 141-147 (2010).

[50] Anbia M., Khazaei M., Ordered Nanoporous Carbon-Based Solid-Phase Microextraction for the Analysis of Nitroaromatic Compounds in Aqueous Samples, *Iran. J. Chem. Chem. Eng.* (IJCCE), **33(4)**: 29-39 (2014).

[51] Aminy M., Barhemmati-Rajab N., Zamzamian S. A., Investigating Effect of CuO and TiO_2 Nano Particles on Tribological Characteristics of Engine Oil, *J. Adv. Mate. Technol.* **3(4)**: 71-76 (2015).

[52] Barhemmati-Rajab N., Mahadevan T., Du J., Zhao W., Thermal Transport Properties Enhancement of Paraffin via Encapsulation into Boron Nitride Nanotube: a Molecular Dynamics Study, *MRS Commun.*, (2020).

[53] Aminy M., Barhemmati-Rajab N., Hadadian A., Vali F., "Design of a Photovoltaic System for a Rural House", *Second Iranian Conference on Renewable Energy and Distributed Generation*, Tehran, 2012,

[54] Babapoor A., Haghighi A., Jokar S. M., Ahmadi Mezjin M., The Performance Enhancement of Paraffin as a PCM During the Solidification Process: Utilization of Graphene and Metal Oxide Nanoparticles, *Iran. J. Chem. Chem. Eng. (IJCCE)*, (2021). [In Press]
doi 10.30492/IJCCE.2020.127799.4135